

Macroporous poly(*N*-isopropyl)acrylamide networks: formation conditions

Cigdem Sayil^a, Oguz Okay^{a,b,*}

^aDepartment of Chemistry, TUBITAK Marmara Research Center, P.O. Box 21, 41470 Gebze, Kocaeli, Turkey

^bDepartment of Chemistry, Istanbul Technical University, Maslak, 80626 Istanbul, Turkey

Received 26 January 2001; received in revised form 9 March 2001; accepted 9 April 2001

Abstract

The formation conditions of macroporous poly(*N*-isopropyl)acrylamide (PNIPA) networks by free-radical crosslinking copolymerization are described. The networks were prepared in water at an initial monomer concentration of 20% using *N,N'*-methylene(bis)acrylamide (BAAm) as the crosslinker. The synthesis parameters varied were the crosslinker concentration and the gel preparation temperature T_{prep} . Depending on these parameters, the variations of the swelling, mechanical and texture properties of the networks were investigated. It was shown that, after passing a critical crosslinker concentration (2–5% BAAM), the network structure changes from homogeneous to heterogeneous ones. Further increase of the crosslinker content increases both the rate of swelling and the porosity of the networks. Heterogeneous PNIPA networks consist of spherical globules called microspheres of 0.1–0.5 μm in diameter aggregated to large, unshaped, discrete clusters with dimensions of a few μm . At 30% BAAM, the structure looks like cauliflowers, typical for a macroporous network. The dependence of the elastic moduli of PNIPA gels on the crosslinker content shows three different regimes depending on the structure of the networks. Increasing T_{prep} from 9 to 50°C at a fixed BAAM content increases both the rate of swelling and the swelling capacity of the networks, while the total porosity decreases. © 2001 Published by Elsevier Science Ltd.

Keywords: Poly(*N*-isopropyl)acrylamide; Macroporous; Swelling

1. Introduction

Gels are crosslinked polymer networks swollen in a liquid medium. The liquid inside the gel allows free diffusion of some solute molecules, while the polymer network serves as a matrix to hold the liquid together. Poly(*N*-isopropyl)acrylamide (PNIPA) gel is a typical temperature sensitive gel exhibiting volume phase transition at approximately 34°C [1,2]. Below this temperature, the gel is swollen and it shrinks as the temperature is raised. The temperature sensitivity of PNIPA gels has attracted great attention in the last years due to both fundamental and technological interests [3–6]. These materials are useful for drug delivery systems, separation operations in biotechnology, processing of agricultural products, sensors and actuators. In these applications, a fast response rate of the hydrogel to the external stimuli is needed. In order to increase the response rate of PNIPA gels, several techniques were proposed:

1. Submicrometer-sized gel particles [7]: Since the rate of response is inversely proportional to the square of the size of the gel [8], small PNIPA gel particles respond to the external stimuli more quickly than bulk gels.
2. Gels having dangling chains [9–11]: Dangling chains in a gel easily collapse or expand upon an external stimulus because one side of the dangling chain is free.
3. Macroporous PNIPA gels: The kinetics of gel volume change involves absorbing or desorbing solvent by the polymer network, which is diffusive process. This process is slow and even slower near the critical point. However, for a network having an interconnected pore structure, absorption or desorption occurs through the pores by convection, which is much faster than the diffusion process that dominates the non-porous gels.

To prepare macroporous PNIPA networks, one idea is to start the NIPA polymerization below the lower critical solution temperature (LCST) of PNIPA and then elevating the temperature above it [12]. Wu et al. [13] synthesized macroporous PNIPA gels above their LCST in the absence or presence of hydroxypropyl cellulose acting as a pore-forming agent. Other idea is to apply a radiation induced

* Corresponding author. Address: Department of Chemistry Istanbul Technical University, Maslak, 80626 Istanbul, Turkey. Tel.: +90-212-2853156; fax: +90-212-2856386.

E-mail address: okayo@itu.edu.tr (O. Okay).

polymerization method [14–16]. Use of inert diluents such as poly(ethylene glycole) during the network formation process was also suggested for the preparation of macroporous PNIPA [17,18]. All of these works, however, only deal with the investigation of the swelling rate of the gels depending on the synthesis parameters and therefore, they fail to explain the formation process of macroporous PNIPA networks. Furthermore, whether the PNIPA networks prepared so far are macroporous or not is also unclear due to the fact that the term macroporous defines a material having a dry state porosity [19].

It is now well understood that a phase separation during the network formation process is mainly responsible for the formation of porous structures in a dried state [19–24]. In order to obtain macroporous structures, a phase separation must occur during the course of the crosslinking process so that the two-phase structure is fixed by the formation of additional crosslinks. Depending on the synthesis parameters, phase separation takes place on a macroscale or on a microscale. In the first case, the gel deswells (or collapses) at the critical point for phase separation and becomes a microsphere, whereas the separated liquid phase remains as a continuous phase in the reaction system (Fig. 1A). As the reaction proceeds, new microspheres are continuously generated due to the successive separation of the growing polymers. Agglomeration of microspheres leads to the formation of a macroporous network consisting of two continuous phases. In the second case, phase separation results in the formation of a dispersion in the reaction system instead of deswelling. Thus, the liquid phase during the gel formation process separates in the form of small droplets inside the gel and it becomes discontinuous (Fig. 1B). Due to slowness of the volume change of the gel sample, the interior of the sample is initially under constant volume condition; further polymerization and crosslinking reactions fix the two-phase structure in the final material. Many studies have been investigated the formation process of macroporous networks derived from the monomers styrene [19–31], acrylamide [32,33], trimethylolpropane trimethacrylate [34], glycidyl methacrylate [35,36] and 2-hydroxyethyl methacrylate [37–40].

The present paper is the first report on the preparation and characterization of macroporous PNIPA networks. Here, we describe the formation conditions of macroporous PNIPA networks by free-radical crosslinking polymerization and

explain their formation process. The crosslinking copolymerization of NIPA was carried out in water using *N,N'*-methylene(bis)acrylamide (BAAm) as the crosslinker. The synthesis parameters varied were the crosslinker concentration and the gel preparation temperature. Depending on these parameters, the variations of the swelling, mechanical and texture properties of PNIPA networks were investigated.

2. Experimental

2.1. Materials

The monomer NIPA (Aldrich), the crosslinker BAAm (Fluka), the initiator ammonium persulfate (APS, Fluka), and the accelerator *N,N,N',N'*-tetramethylethylenediamine (TEMED, Aldrich) were used as received. TEMED stock solution was prepared by dissolving 0.48 ml of TEMED in 10 ml of water. Distilled and deionized water was used for the swelling experiments. For the preparation of the stock solutions and for the hydrogel synthesis, distilled and deionized water was distilled again prior to use and cooled under nitrogen bubbling.

2.2. Copolymerization

PNIPA gels were prepared by free-radical crosslinking copolymerization of NIPA and BAAm in aqueous solutions. The initial monomer concentration was kept constant at 20% (w/v). The polymerization reactions were initiated using 3.5 mM APS and 0.24% (v/v) TEMED. The polymerization time was set to 1 day. Two sets of experiments were carried out. In the first set, the gel preparation temperature (T_{prep}) was kept constant at 22.5°C while the crosslinker (BAAm) concentration was varied between 0.2 and 30 wt% (with respect to monomers). (The monomer mixtures containing higher than 30% BAAm were not soluble in water.) In the second set, the crosslinker concentration was 5 wt% while T_{prep} was varied between 9 and 50°C. It is to be noted that T_{prep} is the temperature of the thermostated water bath in which the PNIPA gels are prepared. According to the previous works, the actual reaction temperature T deviates from the value of T_{prep} due to the exothermic reaction profiles of the crosslinking copolymerization of NIPA. Depending on the surface-to-volume ratio of the reactor as well as on the composition of the reaction mixture, T attains larger values than T_{prep} during the course of the polymerization. The exothermic nature of NIPA polymerization leads to the appearance of turbidity in the gel formation system well below the LCST of PNIPA. The non-isothermal nature of the crosslinking copolymerization of NIPA has been dealt in many papers [41,42]. In our experiments, we fixed the surface-to-volume ratio of the reactors, which were cylindrical glass tubes of 4 mm in diameter and 10 mm in height.

To illustrate the synthetic procedure, we give details for

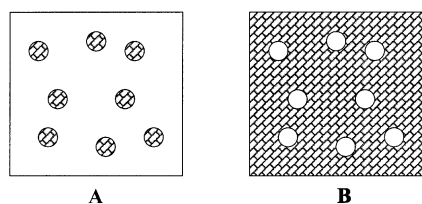


Fig. 1. Schematic representation of phase separation during crosslinking copolymerization on macroscale (A) and microscale (B). White area: liquid phase. Hatched area: gel phase.

the preparation of PNIPA gels with 5% BAAM as the crosslinker: NIPA (1.9 g) and BAAM (0.1 g) were first dissolved in water in a graduated flask of 10 ml in volume and the volume of the monomer solution was completed to 10 ml with distilled water. The solution was purged with nitrogen gas for 20 min and then, portions of this solution, each 1.5 ml, were transferred to glass tubes of 4 mm in diameter. After addition of APS (12 mg) and TEMED stock solution (0.075 ml), the solutions were mixed, the glass tubes were sealed, immersed in a thermostated water bath and the polymerization was conducted for 1 day. After polymerization, the gels were cut into specimens of approximately 10 mm in length and immersed in a large excess of water to wash out any soluble polymers, unreacted monomers and the initiator. The hydrogels after extraction were carefully deswollen in a series of water–acetone mixtures with increasing acetone contents. This solvent exchange process facilitated final drying of the hydrogel samples. They were then washed several times with acetone and dried at room temperature under vacuum to constant weight.

Elemental microanalysis of dried PNIPA networks was performed on a Carlo Erba 1106 elemental analyzer. Table 1 shows the measured elemental composition of some dried PNIPA networks together with the calculated values. Calculations indicate existence of 10–16 wt% water in the network samples even after constant mass drying under vacuum. Such amounts of bounded water were also found before in poly(acrylamide) hydrogels [43]. Moreover, measurements of the diameter of the gels after preparation (D_0) and after drying (D_{dry}) gave the volume fraction of crosslinked polymer after the gel preparation $\nu_2^0((D_{dry}/D_0)^3)$ as 0.24 ± 0.02 , compared to its theoretical value of 0.15, assuming the polymer density as 1.35 g/ml. The ν_2^0 value higher than the theoretical value also indicates the presence of bounded water in the dried gel samples.

2.3. Monomer conversion and gel fraction

The polymerization time for the preparation of PNIPA gels was set to 1 day throughout this study. The gels after preparation were first swollen in water to extract nonpolymerizable or soluble components and then dried to constant mass. The fractional monomer conversion x and the gel fraction W_g were estimated from q_F values, which are the swelling ratios of the networks after their preparation (mass

of gel after preparation/mass of the extracted dry network). q_F relates to x and W_g through the equation:

$$q_F = \left(\frac{100 - \text{Water}\%}{\text{Monomer}\%} \right) \left(\frac{1}{xW_g} \right) \quad (1)$$

where Water% is the residual water content of the network samples and Monomer% the initial monomer concentration (20%). The experiments carried out at various crosslinker contents and temperatures gave $q_F = 4.69 \pm 0.05$. Using this value of q_F values together with the water contents of the networks (Table 1), we calculated using Eq. (1) that the product of the fractional monomer conversion and gel fraction is higher than 90% for all the networks prepared in this study.

2.4. Swelling measurements

The weight and the volume swelling ratios of PNIPA networks were determined in distilled water at 20°C using separate techniques. For the weight swelling ratio measurements, dry PNIPA network samples were immersed in vials filled with distilled water. The vials were set in a temperature-controlled bath of $20 \pm 0.1^\circ\text{C}$. In order to reach the equilibrium degree of swelling, the gels were immersed in water at least for 3 weeks. The mass of the swollen gels was measured on an analytical balance. The weight swelling ratio q_w was calculated as

$$q_w = \frac{\text{swollen mass}}{\text{dry mass}} \quad (2)$$

The volume swelling ratio of PNIPA networks was measured using an image analyzing system consisting of a stereo microscope (Olympus Stereomicroscope SZ), a video camera (TK 1381 EG) and Pentium 2 PC with a data analyzing software (BS-200 BAB). First, the diameters of dry networks were measured. Then, the networks were immersed in vials filled with distilled water of $20 \pm 0.1^\circ\text{C}$. The change in the diameter of the gel samples was followed in situ under microscope. The images were captured at various swelling times and the diameter of the cylindrical specimens were measured using BS-200 BAB data analyzing software. The volume swelling ratio of the gels q_v was

Table 1

Elemental microanalysis results of PNIPA networks of various crosslinker contents. Initial monomer concentration = 20%; $T_{\text{prep}} = 22.5^\circ\text{C}$. Calculations were for water contents given in the last column of the table. The values in parenthesis are calculation results for dry networks

BAAM (wt%)	C (%)		H (%)		N (%)		Water (wt%)
	Found	Calculated	Found	Calculated	Found	Calculated	
2	58.33	56.60 (63.53)	10.17	9.83 (9.67)	10.82	11.14 (12.51)	10.9
10	57.88	55.61 (62.80)	9.79	9.61 (9.41)	11.05	11.48 (12.97)	11.5
20	54.76	51.90 (61.88)	8.79	9.41 (9.09)	10.80	11.36 (13.55)	16.1
30	53.76	52.78 (60.97)	8.48	9.08 (8.76)	12.01	12.23 (14.13)	13.4

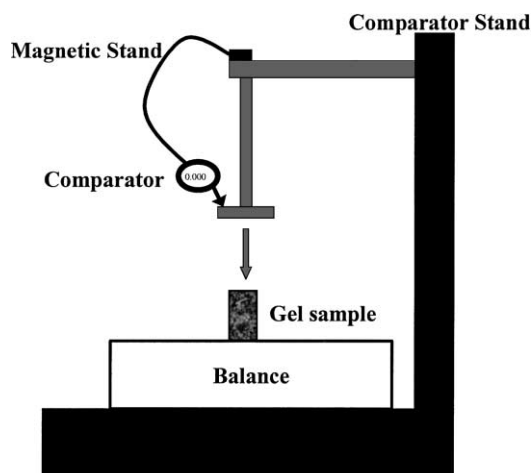


Fig. 2. Uniaxial compression apparatus for measuring stress–strain data on PNIPA gels after preparation.

calculated as

$$q_v = \left(\frac{D}{D_{\text{dry}}} \right)^3 \quad (3)$$

where D and D_{dry} are the diameters of the swollen and dry gels, respectively.

2.5. Mechanical measurements

Uniaxial compression measurements were performed on PNIPA gels after preparation state. All the mechanical measurements were conducted in a thermostated room of $21 \pm 0.1^\circ\text{C}$. The key parts of the apparatus used is shown in Fig. 2.

Briefly, cylindrical gel sample after preparation of 4 mm in diameter and 10 mm in length was placed on a digital balance. A load was transmitted vertically to the gel through a rod fitted with a PTFE end-plate. The force acting on the gel was calculated from the reading of the balance m as $F = mg$, where g is the gravitational acceleration, which is 9.803002 m/s^2 in the place of the measurement (National Metrology Institute of Turkey, UME, TUBITAK, Turkey). The resulting deformation $\Delta l = l_0 - l$, where l_0 and l are the initial undeformed and deformed lengths, respectively, was measured using a digital comparator (IDC type Digimatic Indicator 543-262, Mitutoyo), which was sensitive to displacements of 10^{-3} mm . The force and the resulting deformation were recorded after 20 s of relaxation. The measurements were conducted up to about 20% compression. The deformation ratio α (deformed length/initial length) was calculated as $\alpha = 1 - \Delta l/l_0$. The corresponding stress f was calculated as $f = F/A$, where A is the cross-sectional area of the specimen, $A = \pi r_0^2$, where r_0 is its initial radius.

For uniaxial deformation, the statistical theories of rubber elasticity yield for Gaussian chains an equation

of the form [44]:

$$f = G(\alpha - \alpha^{-2}) \quad (4)$$

where G is the elastic modulus of the samples. Typical stress–strain data correlated according to Eq. (4) are shown in Fig. 3 as filled symbols. Here, the data were from two PNIPA gel samples prepared separately but under identical conditions (monomer concentration = 20%, crosslinker concentration = 5%, gel preparation temperature = 9.5°C). A discrepancy from the linear relationship is obvious at small compressions, which was observed in all gel samples prepared in this study. This deviation from theory can be attributed to the imperfect geometry of the surface of the sample, which decreases the contact area between the PTFE plate and the sample at low compression, and results in relatively high deformations at low stresses. Such deviations were also reported in the literature [45–47]. In order to correct this imperfection, the isotherm was re-drawn by discarding the data at very low strains. The linear portion of the curve was then extrapolated to a value of $-(\alpha - \alpha^{-2})$ at $f = 0$ (dashed curves in Fig. 3) from which the corrected initial length was computed and the deformation ratios were suitably adjusted. The data corrected in this manner are also shown in Fig. 3 as open symbols. The reversibility of the gel deformation was also checked by several samples and found to be reversible.

2.6. Texture determination

The pore sizes, the pore size distribution and the total porosity of PNIPA networks were determined by mercury porosimetry (Micromeritics AutoPore 9220). This technique involves penetration of mercury, at known pressures, into the pores of dry polymer and is based on the Washburn' relationship that the pressure required to force the mercury

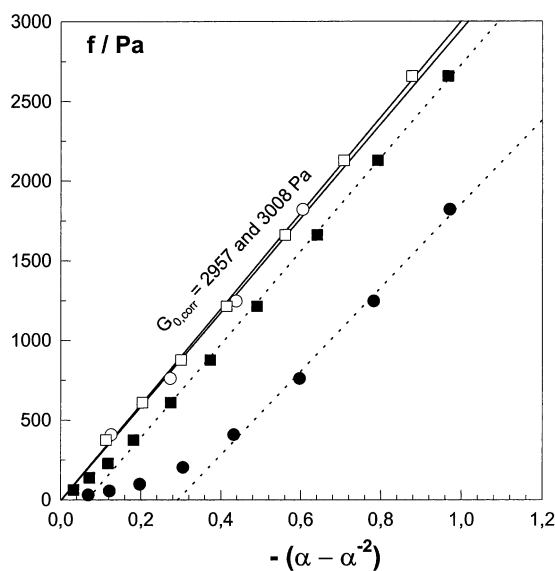


Fig. 3. Typical stress–strain data for two PNIPA gel samples. Monomer concentration = 20%; BAAM concentration = 5%; $T_{\text{prep}} = 9.5^\circ\text{C}$. (●, ■) Uncorrected data; (○, □) corrected data.

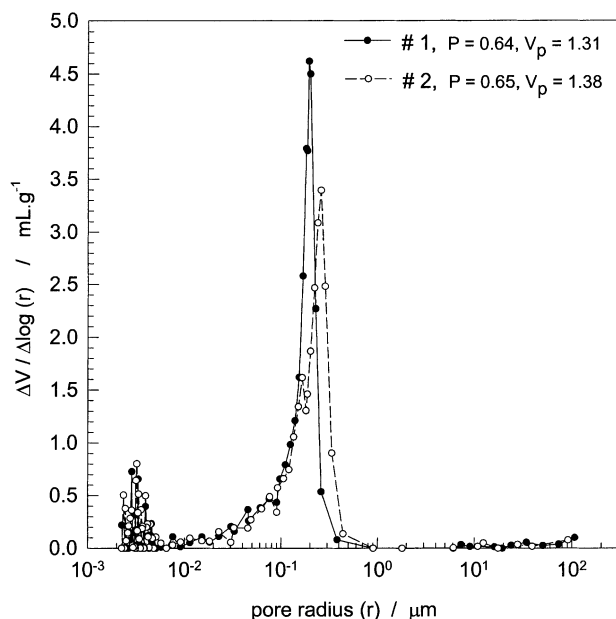


Fig. 4. Differential pore size distributions of two PNIPA network samples taken from the same batch. Monomer concentration = 20%; BAAM concentration = 30%; $T_{\text{prep}} = 22.5^\circ\text{C}$.

into the pores is inversely proportional to their radius [48]. Cumulative pore volume V_p and the total porosity P were estimated from the intruded mercury volumes and the distribution function $\Delta V/\Delta \log r$ was used to express the pore size distribution, where ΔV is the pore volume change when the radius of a cylindrical pore was changed from r to $r - \Delta r$. We obtained reproducible results using PNIPA samples prepared at various conditions. For example, Fig. 4 shows the differential pore size distribution curve of two PNIPA network samples taken from the same batch. The slight shift in average pore diameter values between two successive runs was due to the inefficient mechanical conduction of pressure pulses within the porosimeter.

Scanning electron microscopy studies were carried out at a magnification of $5000\times$ (Jeol JXA-840A).

3. Results and discussion

We discuss the results of our experiments in two sections. In the first section, the formation condition of macroporous PNIPA networks depending on the crosslinker content is described. In the second section, the effect of the gel preparation temperature on the swelling, mechanical and texture properties of PNIPA networks is given.

3.1. Effect of crosslinker concentration

The PNIPA networks were prepared at 20% initial monomer concentration. The gel preparation temperature was set to 22.5°C . The crosslinker (BAAM) concentration was varied between 0.2 and 30%. The gels after preparation were first swollen in water to extract nonpolymerizable or

soluble components and then dried to constant mass. All the swelling experiments were conducted starting from dry state networks.

Results of gravimetric swelling measurements are collected in Fig. 5, which show the weight swelling ratio q_w (swollen mass/dry mass of the network) plotted against the swelling time. In Fig. 6, the equilibrium values of both the weight and volume swelling ratios of the networks are shown as a function of the crosslinker concentration. All the swelling experiments were carried out at $20 \pm 0.1^\circ\text{C}$. As expected, the equilibrium swelling ratio decreases continuously with increasing crosslinker concentration. The dependence of the swelling rate on the crosslinker content shows, however, two different regimes below and above 5% crosslinker BAAM (Fig. 5). Below 5% BAAM, increasing crosslinker concentration decreases the rate of swelling of the networks. This is expected due to the decreasing mesh size of the network with increasing crosslink density, which limits and slows down the diffusion of water molecules into the gel network. However, above 5% BAAM, although the swelling capacities of the networks continue to decrease, the rate of swelling rapidly increases with increasing crosslinker content, which is opposite to what observed below 5% crosslinker (Fig. 5).

Because of the fast swelling of the networks formed above 5% BAAM, their equilibration times in water cannot be measured precisely by the gravimetric technique. Therefore, volumetric measurements were conducted by measuring the diameter of the gel samples, immersed in water, under microscope. Fig. 7 shows the volume swelling ratios of the networks q_v plotted as a function of the swelling time. Large error bars in the figure and the appearance of a maximum in the swelling curve of 20% crosslinker sample are due to the deformation of the originally cylindrical

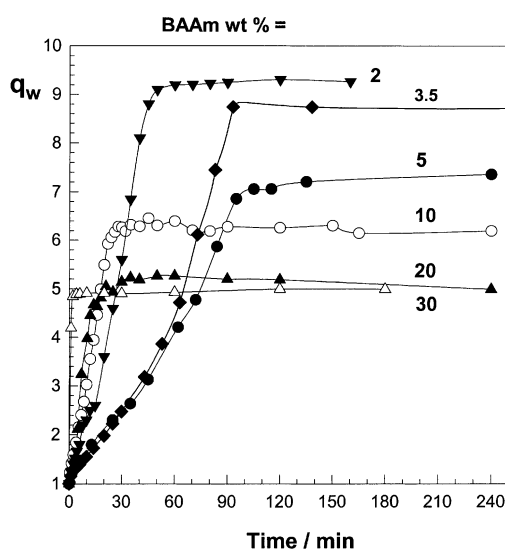


Fig. 5. Weight swelling ratio of PNIPA networks q_w shown as a function of the swelling time. BAAM contents are indicated in the figure. Monomer concentration = 20%; $T_{\text{prep}} = 22.5^\circ\text{C}$.

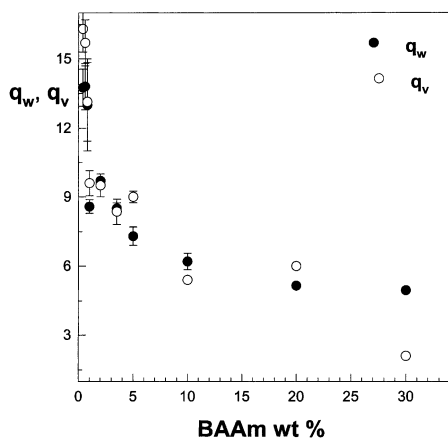


Fig. 6. Equilibrium weight and volume swelling ratios (q_w and q_v , respectively) shown as a function of the crosslinker (BAAm) concentration. Monomer concentration = 20%; $T_{\text{prep}} = 22.5^\circ\text{C}$.

PNIPA networks during their swelling process. In calculating the average value of the volume swelling ratio q_v , the averages of the measurements made at both ends and in the middle of each sample were taken. A series of photographs taken during the swelling process are shown in Fig. 8 and illustrate gel deformation during swelling. When the dry gel sample is immersed in water, it gradually bends; the amount of bending first increases with time, then decreases and finally the gel attains its originally cylindrical shape at swelling equilibrium. Another point is that the gel bends at certain modulated sites, leading to the deformation of the sample. For example, in 10% crosslinker sample, the maximum deformation occurs after 11 min of immersion time in water (Fig. 8). Then, the gel starts to re-homogenize and the original cylindrical shape is recovered after about 30 min, i.e. with the onset of equilibrium swelling. For 20% crosslinker sample, sample deformation was again observed but

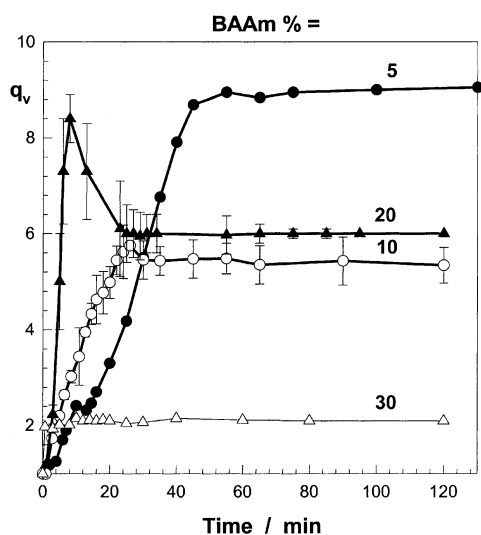


Fig. 7. Volume swelling ratio of PNIPA networks q_v , shown as a function of the swelling time. BAAm contents are indicated in the figure. Monomer concentration = 20%; $T_{\text{prep}} = 22.5^\circ\text{C}$.

with much higher extent (Fig. 8). Here, the maximum deformation appears after 4.5 min, re-homogenization and the equilibrium swelling set in after about 25 min. If the crosslinker content is further increased to 30%, no deformation was observed. This sample attains its equilibrium position in water almost instantaneously within 1 min. One may expect that the deformation and the recovering of the original shape of this sample occur very rapid. Similar deformations were reported before during the swelling and shrinking experiments with PNIPA gels by changing the temperature of solution [49]. A possible explanation of deformation during swelling is associated with the inhomogeneity of PNIPA gels, as will be discussed later. Figs. 7 and 8 also show that the rate of volume swelling increases drastically with increasing crosslinker content from 5 to 30%. The equilibration times of dry networks immersed in water are 30, 25 and about 1 min for 10, 20 and 30% crosslinker samples, respectively.

Increasing swelling rate of the networks with increasing crosslinker content above 5% BAAm can be explained with the formation of heterogeneous structures in PNIPA networks. Indeed, scanning electron micrographs (SEM) shown in Fig. 9 illustrate the development of heterogeneity in the networks depending on the crosslinker content. The numbers in the figure denote the crosslinker contents. At 2% BAAm, the network consists of large polymer domains; the discontinuities between the domains are also large. If the crosslinker content increases from 2 to 5%, the morphology changes drastically and a structure consisting of aggregates of spherical domains appears. We will call these spherical domains as microspheres. The microspheres in 5% crosslinker sample are more or less fused together to form large aggregates. The drastic change of the network structure between 2 and 5% BAAm is reflected by the swelling experiments with increasing swelling rate of the networks (Figs. 5 and 7). As the crosslinker content further increases from 5 to 30% BAAm, the morphology changes from a structure of large aggregates of poorly defined microspheres to one consisting of aggregates of 1–2 μm dimensions of well defined microspheres. The microspheres are about 0.1–0.5 μm in diameter. At 30% BAAm, the structure looks like cauliflowers, typical for a macroporous copolymer network.

From the SEM images, one can identify the pores and the connectivity of the pores in 30% crosslinker sample. Connectivity of pores plays a crucial role in fast weight swelling kinetics of the gels. Water can enter or leave the gel through the interconnected pores by convection. Moreover, increasing internal surface area of the networks also increases the contact area between water and the polymer, which leads to their accelerating volume swelling rates. The PNIPA network with 30% BAAm swells about 60 times faster than the network with 5% crosslinker. As a result, the gel has potential applications in gel sensors and devices.

Fig. 10 shows differential and integral size distributions of pores in PNIPA networks with crosslinker contents between 2 and 30% BAAm recorded using mercury porosimetry. The

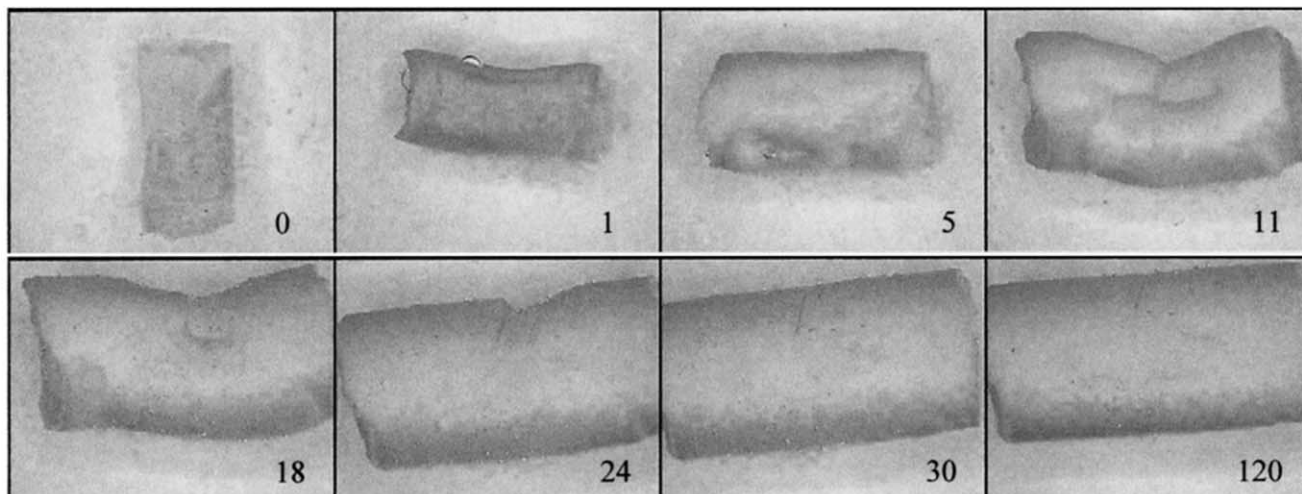
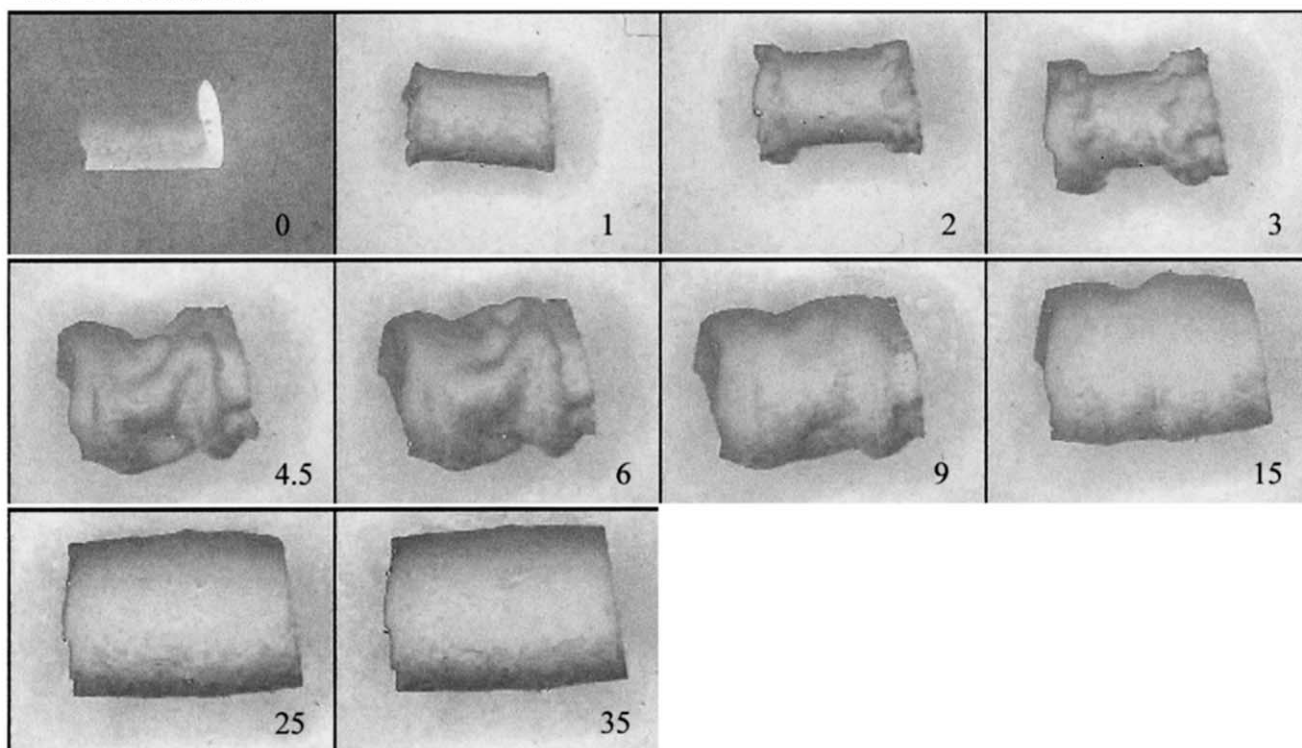
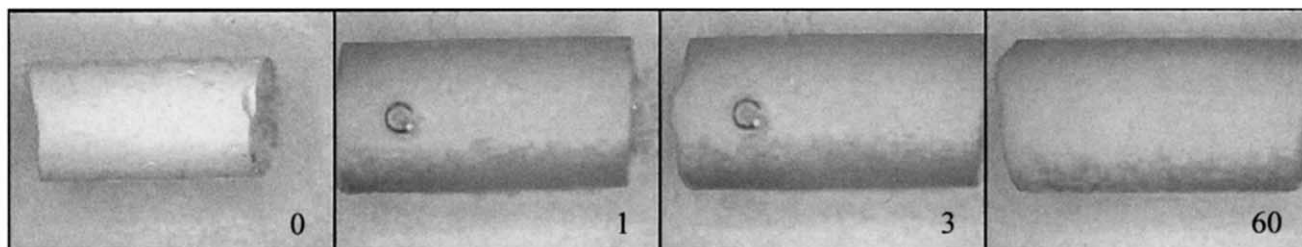
10 % BAAm:**20 % BAAm:****30 % BAAm:**

Fig. 8. A series of photographs taken during the swelling process of PNIPA networks. Swelling times in minutes are given in the photographs. Monomer concentration = 20%; $T_{\text{prep}} = 22.5^\circ\text{C}$.

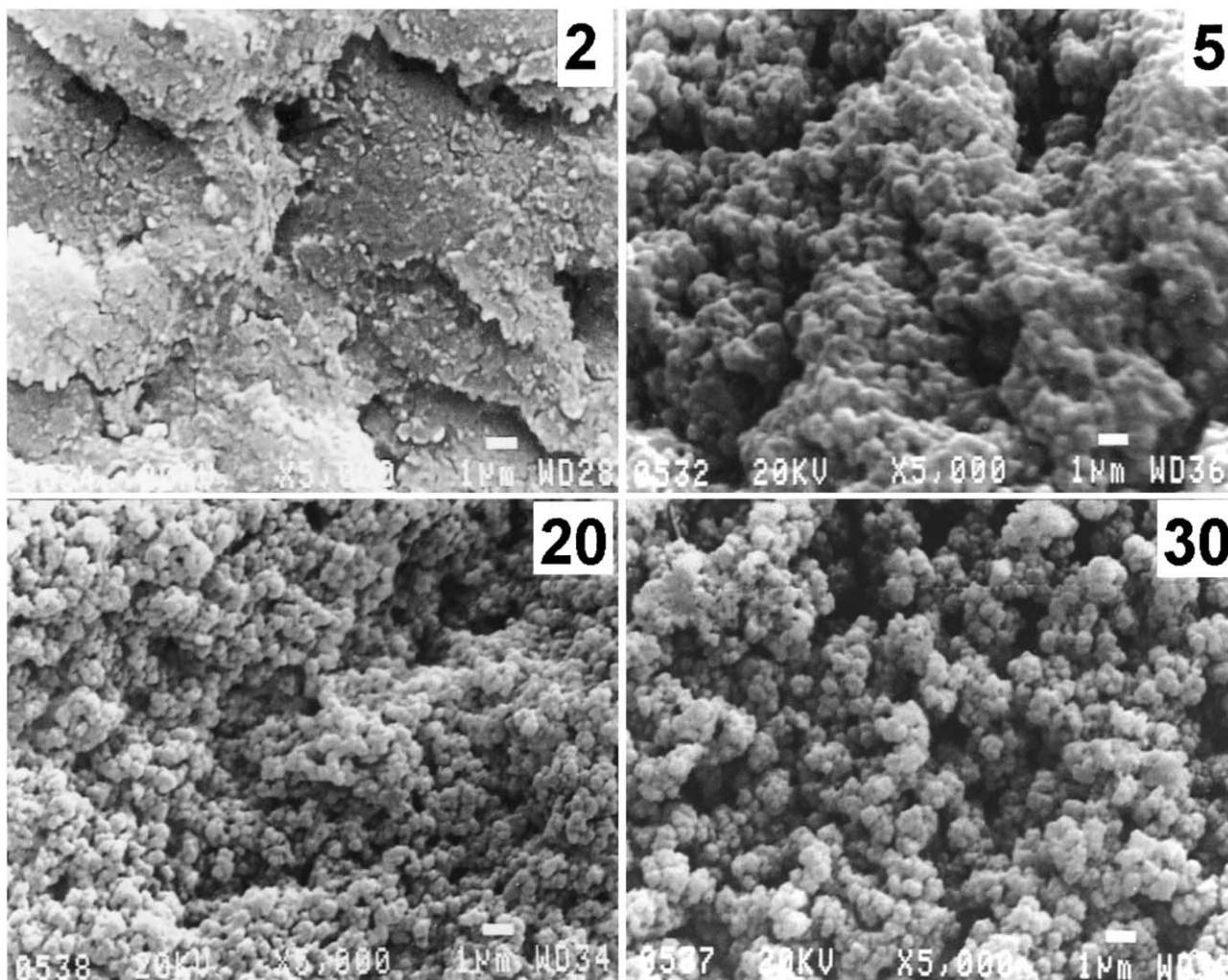


Fig. 9. SEM images of PNIPA networks at $5000\times$ ($1\mu\text{m}$ bar in the lower right corner). BAAM contents are indicated in the figure. Monomer concentration = 20%; $T_{\text{prep}} = 22.5^\circ\text{C}$.

porosity characteristics of the network samples are collected in Table 2. The volume of the pores V_p and the total porosity P of PNIPA networks increase with increasing concentration of BAAM in the feed. As a result, the density of the networks d_0 decreases from 1.19 to 0.47 g/ml with increasing BAAM content (Table 2). From Fig. 10, one can identify three pore size distributions:

1. large pores of about 10–100 μm in radius;
2. macroporous of about 0.1–0.2 μm in radius;
3. micropores of radius less than 60 \AA .

A conventional homogeneous PNIPA gel has the network mesh size in solvents around 5 nm, which corresponds to the micropores of our samples [50]. The micropores and the large pores exist in all network samples studied. However, macropores only exist in 30% crosslinker sample and these pores contribute about 96% of the total porosity of this sample (Table 2). The pore size distribution of macropores is very narrow. Considering the SEM picture of 30% cross-

linker sample, the macropores correspond to the interstices between the microspheres. This indicates that the interstices between the microspheres are accessible to mercury only for the 30% crosslinker sample. For this sample, the total

Table 2

Porosity characteristics of PNIPA networks. Initial monomer concentration = 20%; initiator (APS) concentration = 3.5 mM; accelerator (TEMED) concentration = 0.24% (v/v). T_{prep} : gel preparation temperature; V_p : total volume of pores; d_0 : apparent density; P : total porosity; $V_{p,m}$: total volume of micro- and macropores

T_{prep} ($^\circ\text{C}$)	BAAM (wt%)	V_p (ml/g)	d_0 (g/ml)	P (%)	$V_{p,m}$ (ml/g)
22.5	2	0.10	1.19	0.12	0.02
22.5	5	0.32	0.94	0.30	0.04
22.5	30	1.35	0.47	0.65	1.32
22.5	30 ^a	0.95	0.59	0.56	0.91
9.5	5	0.21	1.06	0.22	0.04
22.5	5	0.32	0.94	0.30	0.04
36.6	5	0.11	1.18	0.12	0.04
50	5	0.09	1.20	0.11	0.04

^a Initial monomer concentration is 10%.

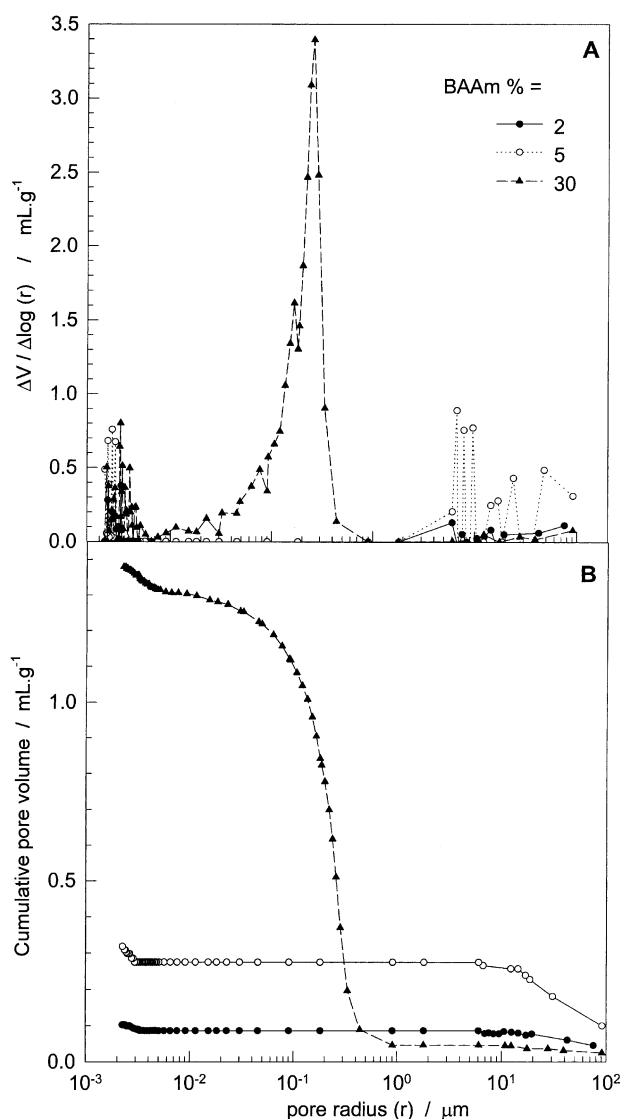


Fig. 10. Pore size distributions of PNIPA networks in (A) differential and (B) integral modes. BAAm contents are indicated in the figure. Monomer concentration = 20%; $T_{\text{prep}} = 22.5^\circ\text{C}$.

porosity calculated from the intruded mercury volume was 65%.

We also tried to increase further the macroporosity of 30% crosslinker sample by decreasing the initial monomer concentration below 20% or, by increasing the crosslinker content above 30%. As is known, the lower the concentration of monomer during gel formation or the higher the crosslinker content, the more heterogeneous is the gel obtained [19]. However, experiments carried out at 10% initial monomer concentration decreased the porosity to 56% (Table 2). Further decrease of monomer concentration to 5% resulted in the formation of weak gels, which collapsed during the drying process. On the other hand, increase of the crosslinker content above 30% was not possible due to the insolubility of BAAm in the aqueous solution.

We propose the following scheme for the formation of heterogeneous PNIPA networks: When the polymerization is initiated by the decomposition of APS and TEMED molecules, the primary radicals formed start to grow by adding the monomer NIPA and the crosslinker BAAm. Initially, the primary molecules contain NIPA units, BAAm units with one vinyl group unreacted (i.e. with pendant vinyl groups) and BAAm units involved in cycles. As the time goes on, more and more primary molecules are formed so that the intermolecular crosslinking reactions between the primary molecules may also occur during the polymerization. Previous works indicate, however, importance of cyclization reactions in free-radical crosslinking copolymerization [51]. For example, in free-radical copolymerization of acrylamide and BAAm at 5% initial monomer concentration, at least 80% of the pendant vinyl groups are consumed by cyclization reactions [52,53]. Thus, cyclization clearly dominates over the intermolecular crosslinking reactions. Since every cycle reduces the coil dimension of the molecules as well as the solvent content inside the coil, the structure of the polymers formed is rather compact and can be considered as clusters. The higher the crosslinker content, the higher is the cyclization density of the clusters, or the lower is their solvent content. When the cyclization density of the clusters exceeds a critical value, they phase separate and form primary particles called microspheres of about 0.1–0.5 μm in diameter. This point corresponds to a BAAm concentration between 2 and 5%. The microspheres are nonporous and constitute the highly crosslinked regions of the network. The agglomeration of the microspheres during crosslinking polymerization through their peripheral pendant vinyl groups and radical ends leads to the formation of large, unshaped, discrete agglomerates of 10–100 μm in diameter, which are further agglomerated to form the final network. Macropores of 0.1–0.2 μm in radius constitute the interstices between the microspheres while the voids between the agglomerates build the large pores in PNIPA networks. Fig. 11 shows a schematic representation of the porous structure of PNIPA networks formed at high crosslinker contents.

Comparing the reactivities of the monomers NIPA and BAAm in free-radical copolymerization, BAAm reactivity is at least twice the NIPA reactivity due to the existence of two vinyl groups on each BAAm molecule. Therefore, the molecules formed earlier should contain more BAAm units and therefore highly crosslinked than those formed later. Due to the rapid consumption of BAAm monomer during polymerization, the density of the clusters will decrease as the monomer conversion increases and, at high conversion degrees, the structure of the clusters will approach to that of the primary molecules. Thus, the microspheres formed earlier (locating in the interior of agglomerates) probably form the highly crosslinked regions of the final material, which are interconnected with loosely crosslinked regions. The presence of these kinds of regions is well known as spatial inhomogeneities. If such an inhomogeneous network

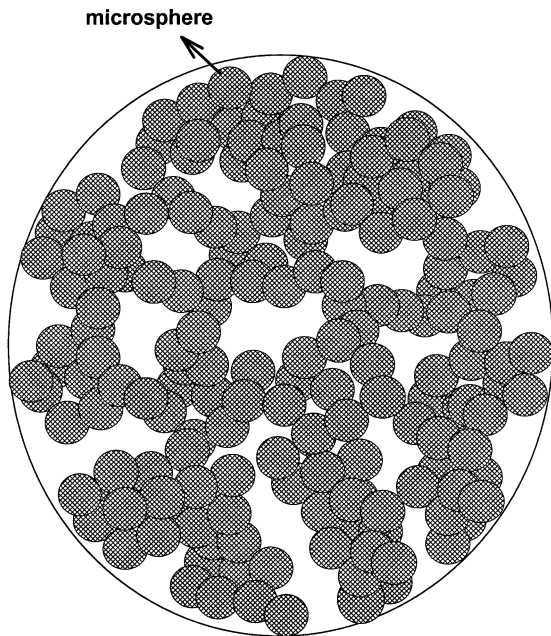


Fig. 11. Schematic representation of the porous structure of PNIPA networks.

is immersed in a good solvent, the loosely crosslinked regions can adjust their orientation to fit a new equilibrium. However, the highly crosslinked regions require much more time to reorganize. As a result, the network will bend toward the parts with lower crosslink density. The deformation of PNIPA networks during swelling can thus be related to the network inhomogeneities. According to Fig. 8, increasing crosslinker content increases the extent of deformation during swelling indicating increasing gel inhomogeneity with increasing crosslinker content. Light scattering measurements indeed show that the extent of gel inhomogeneity increases with increasing crosslinker concentration [54].

The elastic modulus G_0 of PNIPA gels prepared at various crosslinker contents was measured after their preparation. An interpretation of the modulus G_0 of heterogeneous networks is complicated due to the complex character of their deformation process. However, for a homogeneous network of Gaussian chains, G_0 relates to the network crosslink density through the equation [44,55]:

$$G_0 = A \frac{\rho}{M_c} RT v_2^0 \quad (5)$$

where ρ is the polymer density, \bar{M}_c the molecular weight of the network chains, v_2^0 the volume fraction of crosslinked polymer after the gel preparation, R and T in their usual meaning. The front factor A equals to 1 for affine network and $1 - 2/\phi$ for phantom networks, where ϕ is the functionality of the crosslinks.

Fig. 12 shows the moduli of the networks G_0 in kPa plotted as a function of the crosslinker content. Three different regimes can be seen in the figure. (1) At crosslinker contents below 3%: G_0 increases with increasing crosslinker content; (2) between 3 and 5% BAAM: G_0 decreases with

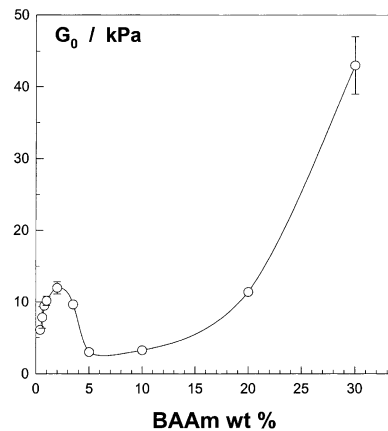


Fig. 12. Elastic modulus G_0 of PNIPA networks after preparation shown as a function of the crosslinker (BAAM) concentration. Monomer concentration = 20%; $T_{\text{prep}} = 22.5^\circ\text{C}$.

increasing crosslinker content; (3) above 5% BAAM: G_0 first remains constant but then increases with the crosslinker content, this increase is rapid between 20 and 30% BAAM.

At a crosslinker content below 3% BAAM, the PNIPA

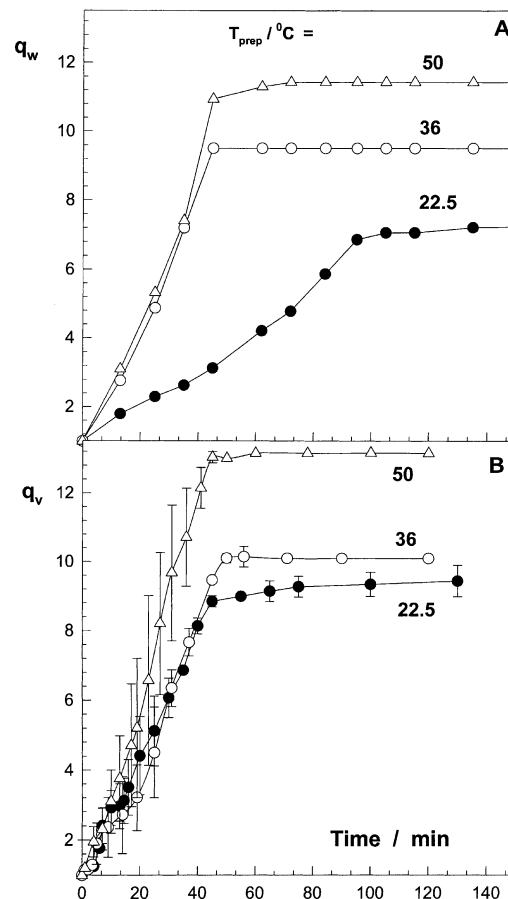


Fig. 13. Weight and volume swelling ratios of PNIPA networks (q_w and q_v , respectively) shown as a function of the swelling time. Gel preparation temperatures (T_{prep}) are indicated in the figure. Monomer concentration = 20%; BAAM = 5%.

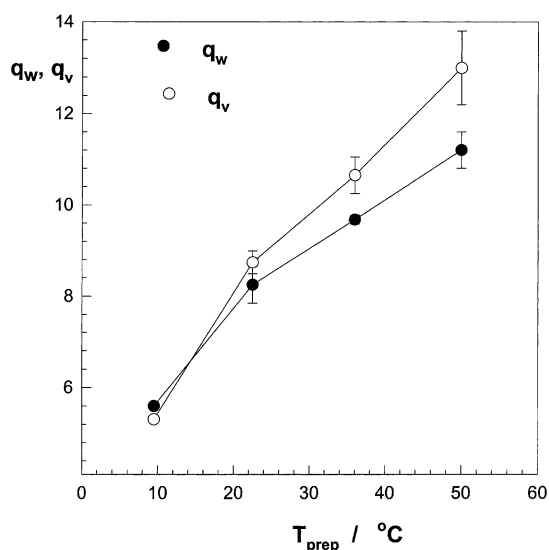


Fig. 14. Equilibrium weight and volume swelling ratios (q_w and q_v , respectively) shown as a function of the gel preparation temperatures T_{prep} . Monomer concentration = 20%; BAAM = 5%.

networks formed are close to the homogeneous limit. Therefore, in accord with the statistical theory of rubber elasticity (Eq. (5)), the elastic behavior in the first region is expected. The rapid decrease of the modulus in the second region (between 3 and 5% BAAM) can be explained with the help of Fig. 9. As seen in this figure, increasing crosslinker content from 2 to 5% changes the network structure drasti-

cally; a network consisting of large polymer domains becomes a heterogeneous network consisting of agglomerates of microspheres. As a result, bending-type deformations become also operative with increasing crosslinker content due to the buckling of the pore walls or of chains connecting the microspheres. This leads to a decrease in G_0 with increasing crosslinker content in the second region. Literature data also indicate that the modulus of a porous material is less than its value for matrix polymer and it decreases as the porosity increases [56–59].

The drastic increase of the modulus at high crosslinker contents in the final region is attributable rather to a change in the state of the polymer than to a change in the porous structure. As seen in Fig. 6, with increasing crosslinker content from 20 to 30%, the volume swelling ratio q_v of the network decreases from 6 to 2 while the weight swelling ratio q_w remains at its limiting value of 5.2. The volume swelling is mainly caused by the solvation of the network chains and thus, it includes the amount of solvent in the network region, while the weight swelling includes the amount of solvent both in network and pore regions [19]. Therefore, decrease of q_v at fixed q_w between 20 and 30% BAAM indicates that the microspheres in 30% crosslinker sample are largely unswollen, which facilitates the condition of attaining the glassy state of this sample after the gel preparation. Thus, one may expect that the PNIPA network passes from rubbery to glassy state between 20 and 30% BAAM, resulting in a rapid increase of the modulus

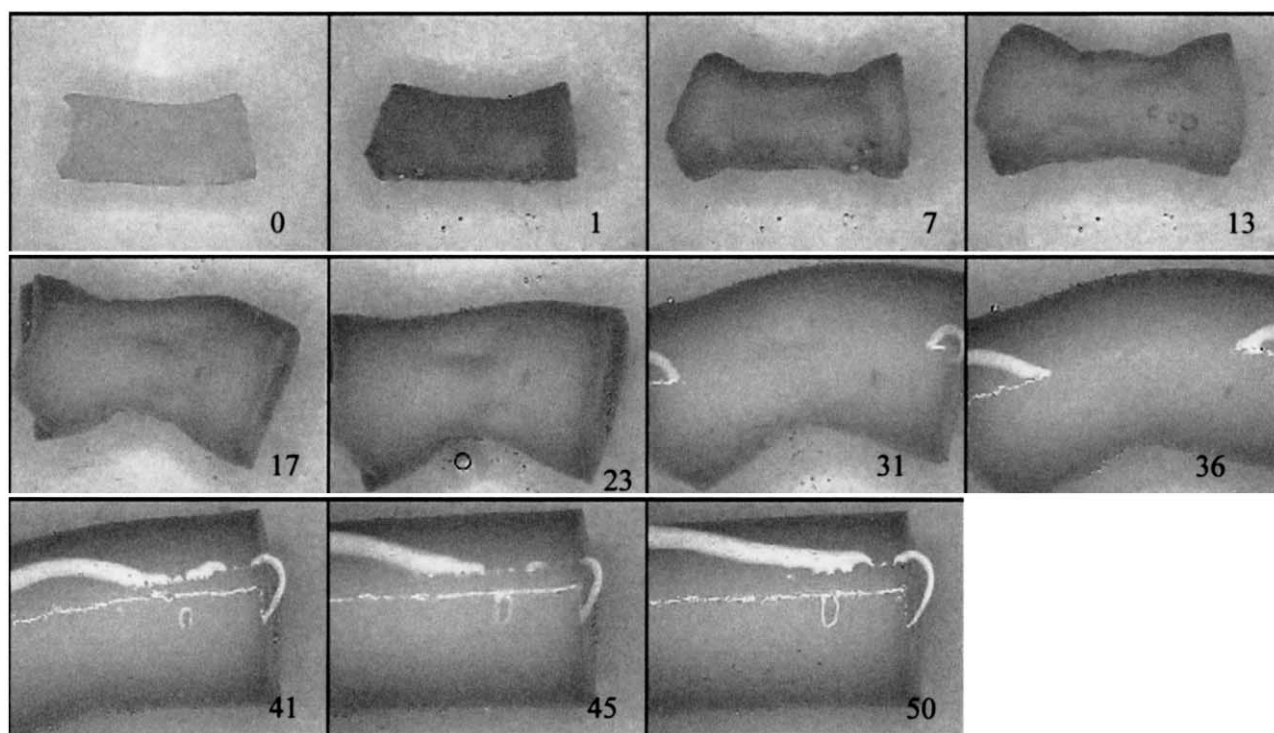


Fig. 15. A series of photographs taken during the swelling process of a PNIPA network sample prepared at 50°C. Swelling times in minutes are given in the photographs. Monomer concentration = 20%; BAAM = 5%.

(Fig. 12). This may also explain the existence of macropores in 30% crosslinker sample. Below 30% BAAM, the voids between the microspheres disappear during drying process due to the cohesional forces between the solvated chains on the microspheres. At 30% BAAM, the microspheres, which are in the glassy state after gel preparation, remain stable during drying so that the macropores become accessible to mercury intrusion in dry state.

3.2. Effect of the gel preparation temperature

In this section, the PNIPA networks were prepared at a crosslinker content of 5%, while the gel preparation temperature T_{prep} was varied. Visually, we observed formation of glassy polymers below 22.5°C whereas opaque gels were obtained above this temperature. Further, opacity increased as T_{prep} is increased. Since the opacity is a result of light scattering from the spatial inhomogeneities of the gel refractive index, these results indicate existence of domains in PNIPA gels in the order of the wavelength of visible light.

Fig. 13 shows the weight and volume swelling ratios of the networks (q_w and q_v , respectively) plotted as a function of the swelling time. In Fig. 14, the equilibrium weight and volume swelling ratios are shown as a function of T_{prep} . As expected [60,61], both the rate of swelling and the equilibrium swelling ratio increase with increasing T_{prep} . Again, sample deformation was observed during the swelling process leading to the large error bars in the volume swelling curves (Fig. 13B). Fig. 15 shows photographs taken from a gel sample prepared at 50°C at various swelling times. Swelling was accompanied with the deformation of the gel sample. The extent of deformation increased with increasing T_{prep} , indicating increasing inhomogeneity in the network structure on raising the gel preparation temperature. The inhomogeneities in PNIPA gels depending on T_{prep} have been extensively investigated using light scattering techniques [62,63]. The results also show that the extent of inhomogeneity steeply increases with increasing T_{prep} for above 23°C [64].

Another point shown in Fig. 14 is that, although both q_w and q_v increase with increasing T_{prep} , the increase of q_v is much rapid than that of q_w . According to the relations between the swelling ratio and the porosity of heterogeneous networks [19,65,66], this indicates a decrease of the porosity with increasing T_{prep} . Indeed, the porosity characteristics of the networks collected in Table 2 show that the porosity of the networks decreases with increasing T_{prep} . This is rather contradictory to our expectation since (a) the PNIPA gels are believed to be more heterogeneous as T_{prep} increases due to the action of water as a poor solvent (pore-forming agent) at elevated temperatures and (b) the opacity of gels formed above 22.5°C indicated existence of phase separated domains of sizes 10^{-1} μm . Fig. 16 shows differential and integral size distribution of pores in PNIPA networks prepared at various temperatures. One can identify

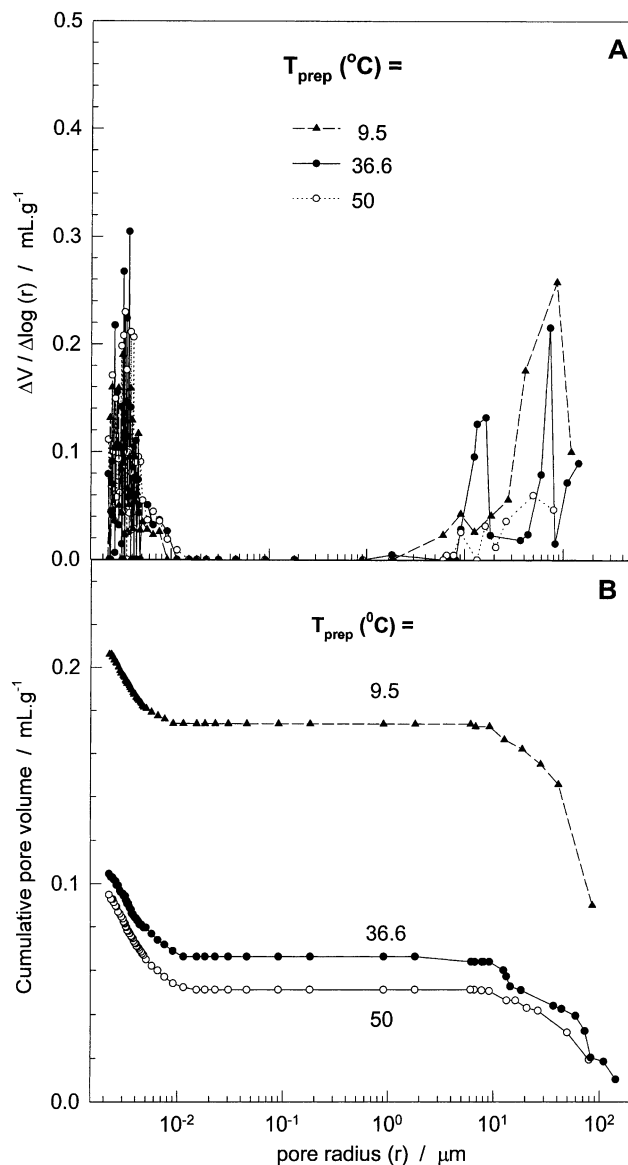


Fig. 16. Pore size distributions of PNIPA networks in (A) differential and (B) integral modes. Gel preparation temperatures T_{prep} are indicated in the figure. Monomer concentration = 20%; BAAM = 5%.

large pores of 10–100 μm in radius and micropores of less than 60 Å in radius. However, macropores of sizes 10^{-1} μm are missing and, an increase of T_{prep} up to 50°C does not induce formation of these pores. The networks prepared at a low temperature mainly consist of large pores. As T_{prep} increases, the volume of large pores decreases while that of micropores remains constant at 0.04 ml/g over the entire range of T_{prep} studied (Table 2).

The results can be explained as follows: At a T_{prep} above the LCST of PNIPA, the phase separation of growing chains causes to the formation of a fine dispersion in the reaction system. However, if T_{prep} is below the LCST, large polymer clusters forming in the system agglomerate with each other leaving large voids between them (Fig. 8). Thus, more ordered structures form as the gel preparation temperature

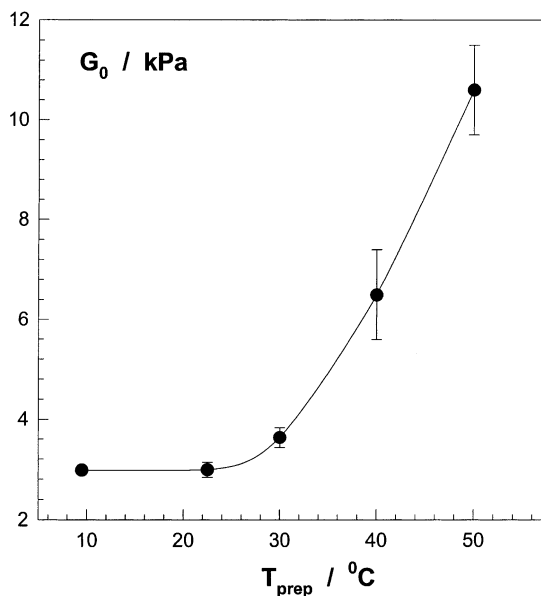


Fig. 17. Elastic modulus G_0 of PNIPA networks after preparation shown as a function of the gel preparation temperatures T_{prep} . Monomer concentration = 20%; BAAM = 5%.

increases, so that the volume of large pores decreases. Appell et al. [50] investigated by Raman spectroscopy the PNIPA gel structure by swelling in water at various temperatures. By using this technique, they were able to distinguish areas of increasing concentration of water, which can be interpreted as the pores. When the swelling temperature is below the LCST of PNIPA, the gel consists of interconnected pores with the size in the order of 75 μm , which corresponds to what we observed in PNIPA networks prepared at low temperatures. In accord with our findings, they also observed disappearance of these large pores above 36°C.

In Fig. 17, the elastic moduli G_0 of the gels are shown as a function of T_{prep} . G_0 remains almost constant up to 30°C but then rapidly increases with increasing T_{prep} , probably due to the decrease of porosity of the networks formed at a high temperature.

4. Conclusions

PNIPA networks were prepared by free-radical crosslinking copolymerization in water at an initial monomer concentration of 20% using BAAM as a crosslinker. The synthesis parameters varied were the crosslinker concentration and the gel preparation temperature T_{prep} . The following conclusions were drawn from the experimental data:

1. After passing a critical crosslinker concentration (2–5% BAAM), the network structure changes from homogeneous to heterogeneous ones. Further increase of the crosslinker content increases both the rate of swelling and the porosity of the networks.

2. Heterogeneous PNIPA networks consist of spherical globules called microspheres of 0.1–0.5 μm in diameter aggregated to large, unshaped, discrete clusters with dimensions of a few μm . Macropores of 0.1–0.2 μm in radius constitute the interstices between the microspheres, while the voids between the agglomerates build the large pores in PNIPA networks. At 30% BAAM, the structure looks like cauliflowers, typical for a macroporous network.
3. The dependence of the elastic moduli of PNIPA gels on the crosslinker content shows three different regimes depending on the structure of the networks.
4. Increasing T_{prep} from 9 to 50°C at a given BAAM content (5%) increases both the rate of swelling and the swelling capacity of the networks, while the total porosity decreases.

References

- [1] Hirokawa T, Tanaka T. *J Chem Phys* 1984;81:6379.
- [2] Hirotsu S. *Adv Polym Sci* 1993;110:1.
- [3] Bar YH, Okano T, Hsu R, Kim SW. *Macromol Chem Rapid Commun* 1987;8:481.
- [4] Doing LC, Hoffman AS. *J Control Release* 1986;4:223.
- [5] Freitas RFS, Cussler EL. *Chem Engng Sci* 1987;42:97.
- [6] Okano T. *Adv Polym Sci* 1993;110:180.
- [7] Oh KS, Oh JS, Choi HS, Bae YC. *Macromolecules* 1998;31:7328.
- [8] Tanaka T, Fillmore DJ. *J Chem Phys* 1979;70:1214.
- [9] Yoshida R, Uchida K, Kaneko Y, Sakai K, Kikuchi A, Sakurai Y, Okano T. *Nature* 1995;374:240.
- [10] Kaneko Y, Sakai K, Kikuchi A, Yoshida R, Sakurai Y, Okano T. *Macromolecules* 1995;28:7717.
- [11] Kaneko Y, Sakai K, Kikuchi A, Sakurai Y, Okano T. *Macromol Symp* 1996;109:41.
- [12] Kabra BG, Gehrke SH. *Polym Commun* 1991;32:322.
- [13] Wu XS, Hoffman AS, Yager P. *J Polym Sci, Part A: Polym Chem* 1992;30:2121.
- [14] Kishi R, Hirasu O, Ichijo H. *Polym Gels Networks* 1997;5:145.
- [15] Chapiro A, Legris C. *Radiat Phys Chem* 1985;28:143.
- [16] Huang X, Unno H, Akehata T, Hirasu O. *J Chem Engng Jpn* 1987;20:123.
- [17] Cicek H, Tuncel A. *J Polym Sci, Part A: Polym Chem* 1998;36:527.
- [18] Zhang X-Z, Zhuo R-X. *Eur Polym J* 2000;36:2301.
- [19] Okay O. *Prog Polym Sci* 2000;25:711.
- [20] Seidl J, Malinsky J, Dusek K, Heitz W. *Adv Polym Sci* 1967;5:113.
- [21] Dusek K. In: Chomppff AJ, Newman S, editors. *Polymer networks: structure and mechanical properties*, New York: Plenum Press, 1971. p. 245–60.
- [22] Guyot A, Bartholin M. *Prog Polym Sci* 1982;8:277.
- [23] Okay O. *Polymer* 1999;40:4117.
- [24] Okay O. *J Appl Polym Sci* 1999;74:2181.
- [25] Cheng CM, Micale FJ, Vanderhoff JW, El-Aasser MS. *J Polym Sci, Polym Chem Ed* 1992;30:235.
- [26] Erbay E, Okay O. *J Appl Polym Sci* 1999;71:1055.
- [27] Ugelstad J, Mork PC, Schmid R, Ellingsen T, Berge A. *Polym Int* 1993;30:157.
- [28] Wang QC, Svec F, Frechet JMJ. *J Polym Sci, Polym Chem Ed* 1994;32:2577.
- [29] Shea KJ, Sasaki DY, Stoddard GJ. *Macromolecules* 1989;22:1722.
- [30] Okay O. *J Appl Polym Sci* 1986;32:5533.

- [31] Hainey P, Huxham IM, Rowatt B, Sherrington DC, Tetley L. *Macromolecules* 1991;24:117.
- [32] Xie S, Svec F, Frechet JMJ. *J Polym Sci A: Polym Chem* 1997;35:1013.
- [33] Shea KJ, Stoddard GJ, Shavella DM, Wakui F, Choate RM. *Macromolecules* 1990;23:4497.
- [34] Rosenberg JE, Flodin P. *Macromolecules* 1986;19:1543.
- [35] Horak D, Labsky J, Pilar J, Bleha M, Pelzbauer Z, Svec F. *Polymer* 1993;34:3481.
- [36] Svec F, Frechet JMJ. *Macromolecules* 1995;28:7580.
- [37] Chirila TV, Chen Y-C, Griffin BJ, Constable IJ. *Polym Int* 1993;32:221.
- [38] Huglin MB, Yip DCF. *Macromolecules* 1992;25:1333.
- [39] Okay O, Gurun C. *J Appl Polym Sci* 1992;46:401.
- [40] Horak D, Lednicky F, Bleha M. *Polymer* 1996;37:4243.
- [41] Gehrke SH, Palasis M, Akhtar MK. *Polym Int* 1992;29:29.
- [42] Champ S, Xue W, Huglin MB. *Macromol Mater Engng* 2000;282:37.
- [43] Durmaz S, Okay O. *Polymer* 2000;41:3693.
- [44] Treloar LRG. *The physics of rubber elasticity*. Oxford: Oxford University Press, 1975.
- [45] Rietsch F, Froelich D. *Polymer* 1975;16:873.
- [46] Froelich D, Crawford D, Rozek T, Prins W. *Macromolecules* 1972;5:100.
- [47] Richards RW, Davidson NS. *Macromolecules* 1986;19:1381.
- [48] Gregg SJ, Sing KSW. *Adsorption, surface area and porosity*, 2nd ed. New York: Academic Press, 1982. p. 116–68.
- [49] Hirose H, Shibayama M. *Macromolecules* 1998;31:5336.
- [50] Appell R, Xu W, Zerda TW, Hu Z. *Macromolecules* 1998;31:5071.
- [51] Funke W, Okay O, Joos-Muller B. *Adv Polym Sci* 1998;136:139.
- [52] Tobita H, Hamielec AE. *Polymer* 1990;31:1546.
- [53] Naghash HJ, Okay O. *J Appl Polym Sci* 1996;60:971.
- [54] Travas-Sejdic J, Eastal AJ. *Polymer* 2000;41:2535.
- [55] Flory PJ. *Principles of polymer chemistry*. Ithaca, NY: Cornell University Press, 1953.
- [56] Wieczorek PP, Ilavsky M, Kolarz BN, Dusek K. *J Appl Polym Sci* 1982;27:277.
- [57] Gent AN, Thomas AG. *J Appl Polym Sci* 1959;1:107.
- [58] Rush KC. *J Appl Polym Sci* 1969;13:2297.
- [59] Horak D, Pelzbauer Z, Bleha M, Ilavsky M, Svec F, Kalal J. *J Appl Polym Sci* 1981;26:411.
- [60] Kayaman N, Kazan D, Erarlan A, Okay O, Baysal BM. *J Appl Polym Sci* 1998;67:805.
- [61] Sayil C, Okay O. *Polym Bull* 2000;45:175.
- [62] Matsuo ES, Orkisz M, Sun S-T, Li Y, Tanaka T. *Macromolecules* 1994;27:6791.
- [63] Shibayama M, Takata S, Norisuye T. *Physica A* 1998;249:245.
- [64] Suzuki Y, Nozaki K, Yamamoto T, Itah K, Nishio I. *J Chem Phys* 1992;97:3808.
- [65] Okay O, Gurun C. *J Appl Polym Sci* 1992;46:421.
- [66] Okay O. *Angew Makromol Chem* 1988;157:1.